An OFDM Carrier Frequency Offset Estimation Scheme with Wide Fractional Offset Estimation Range

C. Yu[1], Y. Lee[2], S. Y. Kim[3], G. I. Jee[4], S. Yoon*[5]

[1,2,5] College of Infomation and Communication Engineering
Sungkyunkwan University
Suwon, Korea
*syoon@skku.edu
[3,4] Department of Electronics Engineering
Konkuk University
Seoul, Korea

ABSTRACT

In this paper, we propose a carrier frequency offset (CFO) estimation scheme which is robust to the fractional CFO variation for orthogonal frequency division multiplexing (OFDM) systems. The proposed scheme first performs the envelope equalization process to convert the offset estimation problem to a carrier estimation problem, and then, estimates the integer and fractional parts of CFO by using periodogram of the received signal. Especially, in the estimation stage for fraction CFO, the ratio of the square-roots of periodograms is employed enlarging the estimation range of the stage than that of the conventional scheme. Numerical results demonstrate that the proposed scheme has better estimation performance than the conventional scheme for wider fractional CFO range in various channel conditions.

Keywords: Estimation, carrier frequency offset, orthogonal frequency division multiplexing (OFDM), periodogram.

1. Introduction

In wireless communication systems including wireless local area network (WLAN) [1], wireless metropolitan area network (WMAN), and digital video broadcasting (DVB) systems, the orthogonal frequency division multiplexing (OFDM) modulation has been widely used due to its high spectral efficiency and immunity to multipath fading [2]. However, the OFDM system is very sensitive to the carrier frequency offset (CFO) caused by Doppler shift [3] and oscillator instabilities [4]. Thus, the CFO estimation is one of the most important technical issues in OFDM systems.

Several schemes [5]-[8] have been proposed to estimate the CFO of OFDM signals. In [5], a CFO estimation scheme using a training symbol with two identical halves was proposed, whose estimation range equals to the subcarrier spacing. A novel CFO estimation scheme that utilizes a training symbol with more than two identical parts was proposed in [6], increasing the estimation range to twice that of the scheme in [5]. With the maximum-likelihood (ML) criterion, in [7], an optimal CFO estimation scheme was derived using the same training symbol as in [6].

Recently, in [8], an interesting CFO estimation scheme was proposed using an envelope equalization process (EEP) and periodogram operations. The scheme can be applied to a training symbol with arbitrary structure having the estimation range as large as the bandwidth of the OFDM signal by estimating the integer and fractional parts of the CFO (IFO and FFO) in each dedicated estimation stages, respectively. However, the performance of the scheme is very sensitive to the variation of the FFO distributed uniformly over $[-0.5, 0.5]$. Although the scheme in [8] employs an additional estimation stage to estimate the residual CFO (RFO), the performance sensitivity to the FFO variation still remains.

In this paper, we propose an improved periodogram-based CFO estimation scheme robust to the FFO variation for OFDM systems. The proposed scheme has wider FFO estimation range and numerical

results demonstrate that the proposed scheme has better estimation performance than the conventional scheme in [8] for wider FFO range.

2. System model

The nth baseband OFDM sample x_n of a training symbol can be expressed as

$$x_n = \sum_{k=0}^{N-1} c_k e^{j2\pi kn/N}, \text{ for } n = 0,1,...,N-1, \qquad (1)$$

where c_k is the data symbol for the kth subcarrier and N is the size of inverse fast Fourier transform (IFFT). Then, the nth received OFDM sample r_n can be expressed as

$$r_n = \sum_{m=0}^{L-1} h_m x_{n-m} e^{j2\pi \varepsilon n/N} + w_n, \qquad (2)$$

where ε is the FO normalized by the subcarrier spacing whose integer and fractional parts are denoted by ε_I ($\varepsilon_I \in \{-N/2, -N/2+1, ..., N/2-1\}$) and ε_f ($\varepsilon_f \in [-0.5, 0.5)$), respectively, h_m is the channel coefficient of the mth path of the multipath channel with length of L, and w_n is the zero-mean complex additive noise [9], [10].

At the receiver, we perform the EEP with a factor ρ_n defined by $x_n^*/|x_n|^2$ as in the scheme in [8], and then, the nth output sample r_n' of EEP can be expressed as

$$\begin{aligned} r' &= r_n \cdot \rho_n \\ &= \left[\sum_{m=0}^{L-1} h_m x_{n-m} e^{j2\pi \varepsilon n/N} + w_n \right] \rho_n \\ &= h_0 x_n e^{j2\pi \varepsilon n/N} \frac{x_n^*}{|x_n|^2} + \sum_{m=1}^{L-1} h_m x_{n-m} e^{j2\pi \varepsilon n/N} \rho_n + w_n \rho_n \\ &= h_0 e^{j2\pi \varepsilon n/N} + w_n', \end{aligned} \qquad (3)$$

where $(\cdot)^*$ represents the complex conjugation and $w_n' = \sum_{m=1}^{L-1} h_m x_{n-m} e^{j2\pi \varepsilon n/N} \rho_n + w_n \rho_n$. From Eq. 3,

we can see that the CFO estimation problem is converted into the frequency (ε) estimation problem for a single tone complex sinusoidal signal, which is independent from the structure of the training symbol.

3. Proposed scheme

The CFO estimation process of the scheme in [8] consists of three steps: IFO, FFO, and RFO estimation steps. In [8], the estimates $\hat{\varepsilon}_I$, $\hat{\varepsilon}_f$, and $\hat{\varepsilon}_r$ of the IFO, FFO, and RFO, respectively, are obtained as

$$\hat{\varepsilon}_I = \arg\max_{f_k} \left[|I(f_k)|^2 + |I(f_k+1)|^2 \right], \qquad (4)$$

$$\hat{\varepsilon}_f = \frac{|I(\hat{\varepsilon}_I+1)|}{|I(\hat{\varepsilon}_I)| + |I(\hat{\varepsilon}_I+1)|}, \qquad (5)$$

and

$$\hat{\varepsilon}_r = \frac{|I(\hat{\varepsilon}_I+\hat{\varepsilon}_f+0.5)| - |I(\hat{\varepsilon}_I+\hat{\varepsilon}_f-0.5)|}{2(|I(\hat{\varepsilon}_I+\hat{\varepsilon}_f+0.5)| + |I(\hat{\varepsilon}_I+\hat{\varepsilon}_f-0.5)|)}, \qquad (6)$$

respectively, where $f_k = -\dfrac{N}{2} + k$ ($k \in \{0,1,...,N-1\}$) is the IFO candidate and $|I(z)|^2$ is the periodogram of r_n' defined by $|I(z)|^2 = \left| \sum_{n=0}^{N-1} r_n' e^{-j2\pi zn/N} \right|^2$. Then, the scheme in [8] yields estimate $\hat{\varepsilon}$ as $\hat{\varepsilon}_I + \hat{\varepsilon}_f + \hat{\varepsilon}_r$.

Figure 1 shows the values of $\hat{\varepsilon}_f + \hat{\varepsilon}_r$ as a function of $\varepsilon - \hat{\varepsilon}_I$ in the absence of channel and noise. From the figure, we can see that the scheme in [8] cannot estimate $\varepsilon - \hat{\varepsilon}_I$ even in the absence of channel and noise when $\varepsilon - \hat{\varepsilon}_I < -0.3$ and $1.3 < \varepsilon - \hat{\varepsilon}_I$ (i.e., the estimation range of the FFO and RFO estimation scheme in [8] is $-0.3 \le \varepsilon - \hat{\varepsilon}_I \le 1.3$).
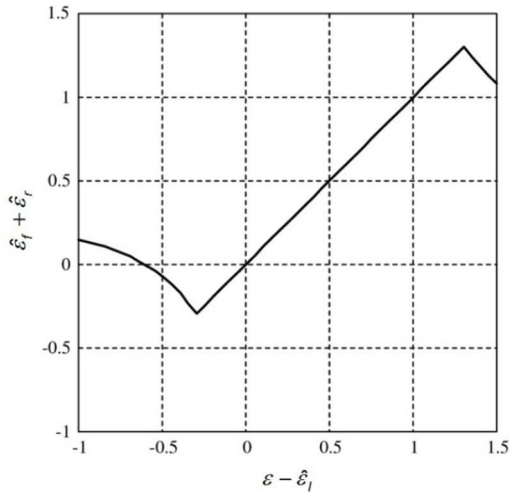
Figure 1. $\hat{\varepsilon}_f + \hat{\varepsilon}_r$ versus $\varepsilon - \hat{\varepsilon}_l$ for the scheme in [8].

Figure 2 shows the IFO metric normalized to $N^2 |h_0|^2$ as a function of f_k and $f \in [-N/2, N/2)$ for $\varepsilon_l = 1$, $\varepsilon_f = 0.4$, and N=8 when the noise is absent, where '∘' represents the IFO metric value corresponding to each integer f_k. Since the FFO and RFO estimation range of the scheme in [8] is $-0.3 \leq \varepsilon - \hat{\varepsilon}_l \leq 1.3$, the scheme in [8] requires an exact IFO estimate (i.e., $\hat{\varepsilon}_l = 1$) to enable the FFO

and RFO estimation scheme in [8] to compensate for the FO $\varepsilon - \hat{\varepsilon}_l$. However, from the figure, we can see that the IFO metric value for $f_k = 0$ is as large as that for $f_k = 1$, and thus, the IFO metric Eq. 4 could yield an incorrect estimate under the influence of noise and channel. In this paper, we propose an FFO estimation scheme with a wide estimation range, allowing the FO to be compensated even though the IFO estimation step fails to provide a correct estimate, which would improve the overall CFO estimation performance.

Assuming that the channel is constant over one OFDM training symbol in the time domain and ignoring the noise term w'_n, we can see that the channel coefficient h_0 can be removed by taking the ratio of square roots of periodograms $I_s(\hat{\varepsilon}_l)$ and $I_s(\hat{\varepsilon}_l + 1)$ as

$$\frac{I_s(\hat{\varepsilon}_l)}{I_s(\hat{\varepsilon}_l + 1)} = \frac{h_0 \cdot \dfrac{1 - e^{j2\pi(\varepsilon - \hat{\varepsilon}_l)}}{1 - e^{j2\pi(\varepsilon - \hat{\varepsilon}_l)/N}}}{h_0 \cdot \dfrac{1 - e^{j2\pi(\varepsilon - \hat{\varepsilon}_l)}e^{-j2\pi}}{1 - e^{j2\pi(\varepsilon - \hat{\varepsilon}_l)/N}e^{-j2\pi/N}}}$$
$$= \frac{1 - e^{j2\pi(\varepsilon - \hat{\varepsilon})/N}e^{-j2\pi/N}}{1 - e^{j2\pi(\varepsilon - \hat{\varepsilon})/N}},$$
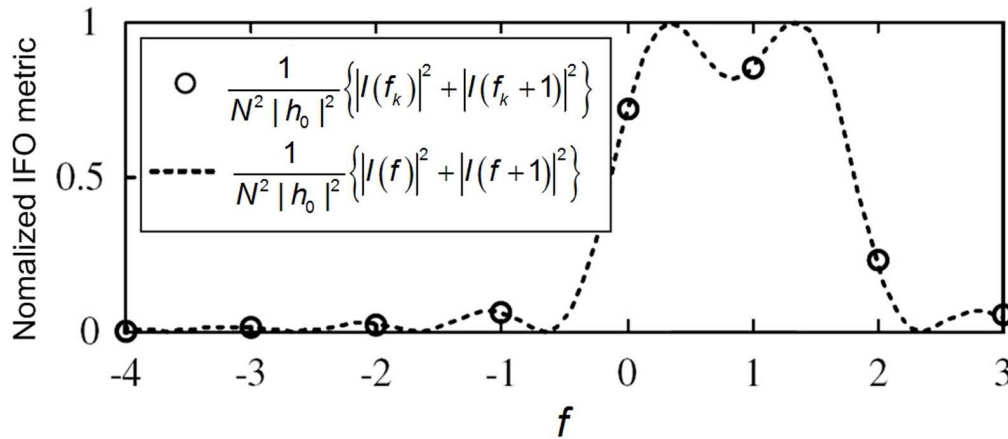(7)

Figure 2. IFO metric normalized to $N^2 |h_0|^2$ as a function of f_k and $f \in [-N/2, N/2)$ when $\varepsilon_l = 1$, $\varepsilon_f = 0.4$, $N = 8$, and the noise is absent.

where $|I_s(z)|^2$ is the periodogram of $h_0 e^{j2\pi\varepsilon n/N}$. Then, we can rewrite Eq. 7 as

$$e^{j2\pi(\varepsilon-\hat{\varepsilon}_I)/N} = \frac{1-I_s(\hat{\varepsilon}_I)/I_s(\hat{\varepsilon}_I+1)}{e^{-j2\pi/N}-I_s(\hat{\varepsilon}_I)/I_s(\hat{\varepsilon}_I+1)}. \qquad (8)$$

Thus, we can obtain the estimate $\hat{\varepsilon}'_f$ as

$$\hat{\varepsilon}'_f = N \cdot \frac{\angle\left(\dfrac{1-M(\hat{\varepsilon}_I)}{e^{-j2\pi/N}-M(\hat{\varepsilon}_I)}\right)}{2\pi}, \qquad (9)$$

where $M(\hat{\varepsilon}_I) = I_s(\hat{\varepsilon}_I)/I_s(\hat{\varepsilon}_I+1)$ and $\angle z$ represents the angle of a complex number z. Considering that $-\pi \leq \angle z \leq \pi$ for a complex number z, we can see that $-\dfrac{N}{2} \leq \hat{\varepsilon}'_f = \dfrac{N}{2\pi}\angle\left(\dfrac{1-M(\hat{\varepsilon}_I)}{e^{-j2\pi/N}-M(\hat{\varepsilon}_I)}\right) \leq \dfrac{N}{2}$,

and thus, the estimation range of the proposed FFO scheme is obtained as $[-N/2, N/2]$ in the absence of channel effect and noise. In the practical case, however, the proposed scheme would have the smaller estimation range than the ideal case of $[-N/2, N/2]$ due to the fading channel and noise. For IFO and RFO estimation steps, we employ Eqs. 4 and 6, respectively.

4. Numerical results

The estimation performance of the proposed and conventional [8] schemes are compared in terms of the frequency offset acquisition probability defined as the probability that the difference between ε and $\hat{\varepsilon}_I + \hat{\varepsilon}'_f$ (or $\hat{\varepsilon}_I + \hat{\varepsilon}_f$) is within the estimation range of the RFO estimation step -0.5 ~0.5. For simulations, we consider the OFDM symbols with 64 subcarriers and 8 guard interval samples and Rayleigh fading channels with an exponential power delay profile with four taps with an equal tap spacing of two samples. The power ratio of the first fading tap to the last fading tap is set to 20 dB. The channel coefficient is time varying with maximum Doppler shift of 266 Hz. The signal-to-noise ratio (SNR) is defined as σ_s^2/σ_w^2, where σ_s^2 and σ_w^2 are variance of the signal and

noise components defined by $E\left\{\left|\sum_{m=0}^{L-1} h_m x_{n-m}\right|^2\right\}$ and $E\left\{|w_n|^2\right\}$, respectively, and $E\{\cdot\}$ is the statistical expection.

Figures 3 and 4 show the frequency offset acquisition probabilities of the proposed and conventional (denoted by Ren) schemes as a function of $\varepsilon - \hat{\varepsilon}_I$ over the additive white Gaussian noise (AWGN) channel, when SNRs are set to 5 and 25 dB, respectively. Also, Figures 5 and 6 show the frequency offset acquisition probabilities over the Rayleigh fading channels when SNRs are set to 5 and 25 dB, respectively. From the figures, we can see that the conventional scheme has the estimation range of $-0.3 \leq \varepsilon - \hat{\varepsilon}_I \leq 1.3$, regardless of the channel and the value of SNR. On the other hand, the proposed scheme is found to have a better frequency offset acquisition probability in a wider range of $\varepsilon - \hat{\varepsilon}_I$ compared with the conventional scheme: Specifically, the proposed scheme always guarantees a reliable estimation performance in the range of $-1 < \varepsilon - \hat{\varepsilon}_I < 2$, and moreover, in the range of $\varepsilon - \hat{\varepsilon}_I < -1$ and $2 < \varepsilon - \hat{\varepsilon}_I$, the frequency offset acquisition probability increases as the value of SNR increases.
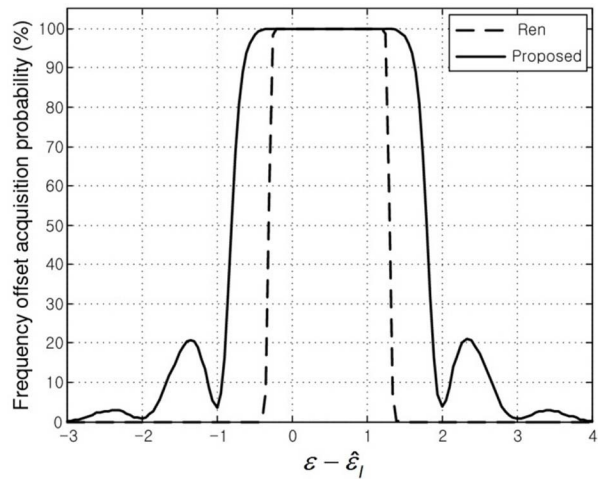

Figure 3. Frequency offset acquisition probability of the proposed and conventional schemes over AWGN channels when SNR = 5 dB.
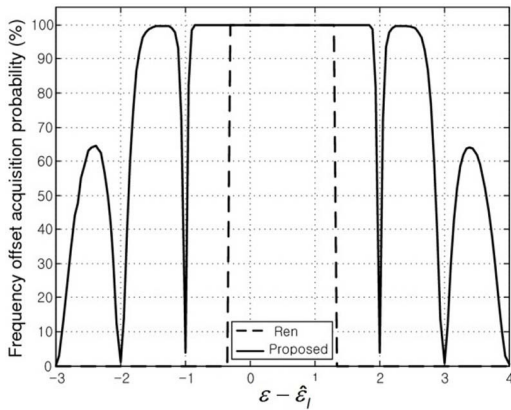
Figure 4. Frequency offset acquisition probability of the proposed and conventional schemes over AWGN channels when SNR = 25 dB.
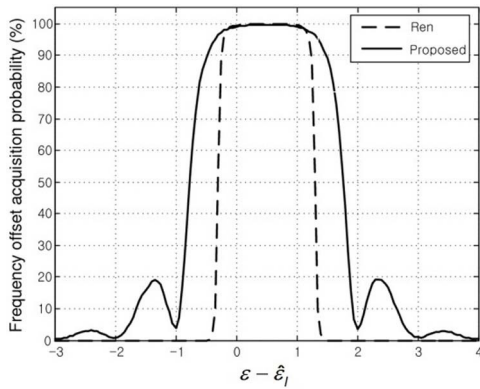

Figure 5. Frequency offset acquisition probability of the proposed and conventional schemes over Rayleigh fading channels when SNR = 5 dB.
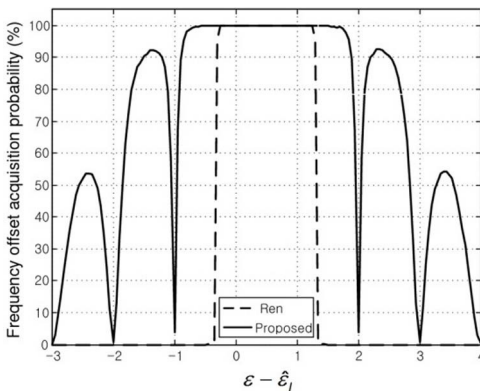

Figure 6. Frequency offset acquisition probability of the proposed and conventional schemes over Rayleigh fading channels when SNR = 25 dB.

Figures 7 and 8 show the frequency offset acquisition probabilities of proposed and conventional schemes as the function of SNR over the AWGN and Rayleigh fading channels, respectively, when $\varepsilon = 1.3$. From the figures, we also can see that the performance of the proposed scheme is better than that of the conventional scheme in the low SNR range and becomes similar as the value of SNR increases.

Since the ambient noise often exhibits impulsive non-Gaussian nature due to moving obstacles, car ignitions, and lightning in the atmosphere [11], we also compare the frequency offset acquisition of the proposed and conventional schemes in non-
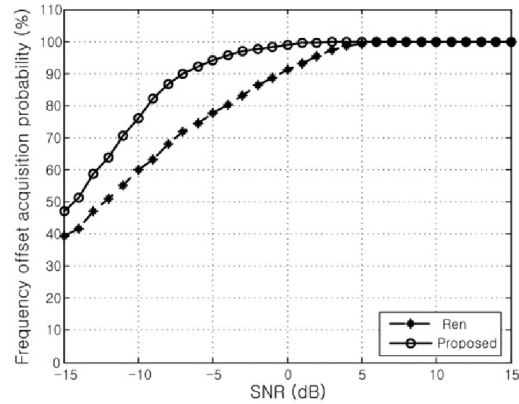

Figure 7. Frequency offset acquisition probability of the proposed and conventional schemes over AWGN channels when $\varepsilon = 1.3$.
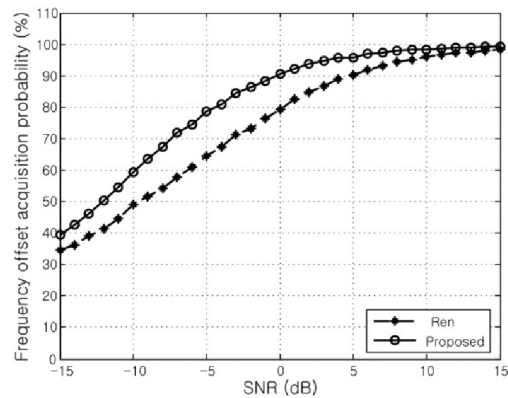

Figure 8. Frequency offset acquisition probability of the proposed and conventional schemes over Rayleigh fading channels when $\varepsilon = 1.3$.

Gaussian noise environments. The non-Gaussian noise is often modeled as Cauchy noise [12]. Since the variance is not defined in Cauchy noise, we employ geometric SNR (G-SNR), which provides the characterization of the relative strength between the signal and noise [13] as $\text{G-SNR} = \sigma_s^2 / (2C\gamma^2)$, where

$C = \exp\left\{ \lim_{b\to\infty} \left(\sum_{a=1}^{b} 1/a - \ln b \right) \right\} \cong 1.78$ is the exponential of the Euler constant, and γ is the dispersion parameter, which is set to 1 in this paper.

Figures 9 and 10 show the frequency offset acquisition probabilities of the proposed and

conventional schemes in non-Gaussian noise environments. From the figures, we can confirm that the proposed scheme has wider estimation range than the conventional scheme in non-Gaussian noise environments as well.

5. Conclusion

In this paper, we have proposed a periodogram-based CFO estimation scheme for OFDM systems. The FFO estimation step of the proposed scheme has the wider estimation range compared with that of the conventional scheme removing the effect of channel effectively. From numerical results, we have confirmed that the proposed scheme has better frequency offset acquisition probability performance than the conventional scheme for wider range of FFO.
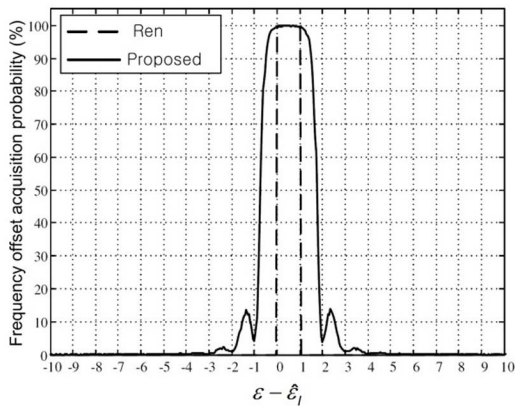

Figure 9. Frequency offset acquisition probability of the proposed and conventional schemes in the presence of non-Gaussian noise when G-SNR = 5 dB.
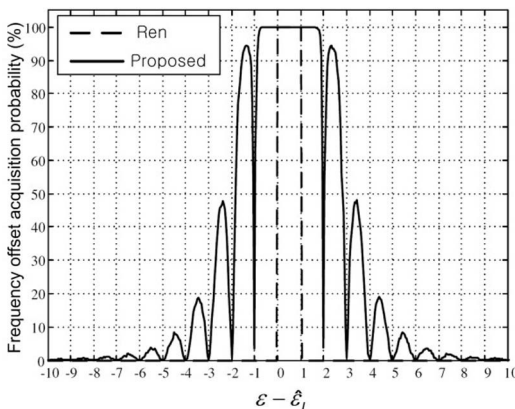

Figure 10. Frequency offset acquisition probability of the proposed and conventional schemes in the presence of non-Gaussian noise when G-SNR = 25 dB.

References

[1] J. Sánchez et al., "Mean receiver power prediction for indoors 802.11 WLANs using the ray tracing technique," Journal of Applied Research and Technology, vol. 5, no. 1, pp. 33-48, 2007.

[2] M. Morelli et al., "Synchronization techniques for orthogonal frequency division multiple access (OFDMA): a tutorial review," Proc. IEEE, vol. 95, no. 7, pp. 1394-1427, 2007.

[3] H.-J. Kwak and G.-T. Park, "Study on the mobility of service robots," International Journal of Engineering and Technology Innovation, vol. 2, no. 2, pp. 13-28, 2012.

[4] R. V. Nee and R. Prasad, "OFDM for wireless multimedia communications", Boston, MA: Artech House, 2000.

[5] T. M. Schmidl and D. C. Cox, "Robust frequency and timing synchronization for OFDM," IEEE Trans. Commun., vol. 45, no. 12, pp. 1613-1621, 1997.

[6] S. Chang and E. J. Powers, "Efficient frequency-offset estimation in OFDM-based WLAN systems," Electron. Lett., vol. 39, no. 21, pp. 1554-1555, 2003.

[7] M.-H. Cheng and C.-C. Chou, "Maximum-likelihood estimation of frequency and time offsets in OFDM systems with multiple sets of identical data," IEEE Trans. Sig. Process., vol. 54, no. 7, pp. 2848-2852, 2006.

[8] G. Ren et al., "An efficient frequency offset estimation method with a large range for wireless OFDM systems," IEEE Trans. Veh. Technol., vol. 56, no. 4, pp. 1892-1895, 2007.

[9] D. Vybiral et al., "Devices for position detection," Journal of Vibroengineering, vol. 13, no. 3, pp. 531-535, 2011.

[10] S. Ginzburg et al., "Design and implementation of an indoor localization system for the omnibot omni-directional platform," Trans. Canadian Society for Mechanical Engineering, vol. 33, no. 4, pp. 715-729, 2011.

[11] P. Toro and M. G. Sanchez, "A study of the correlation between horizontal and vertical polarizations of impulsive noise in UHF," IEEE Trans. Veh. Technol., vol. 56, no. 5, pp. 2844–2849, 2007.

[12] P. Tsakalides and C. L. Nikias, "Maximum likelihood localization of sources in noise modeled as a stable process," IEEE Trans. Sig. Process., vol. 43, no. 11, pp. 2700-2713, 1995.

[13] X. Ma and C. L. Nikias, "Parameter estimation and blind channel identification in impulsive signal environments," IEEE Trans. Sig. Process., vol. 43, no. 12, pp. 2884-2897, 1995.